International Journal of Minerals, Metallurgy and Materials
Volume 21, Number 8, August 2014, Page 832
DOI: 10.1007/s12613-014-0978-6

Production of HfO_2 thin films using different methods: chemical bath deposition, SILAR and sol–gel process

İ.A. Kariper

Education Faculty, Erciyes University, 38039, Kayseri, Turkey

(Received: 3 December 2013; revised: 25 February 2014; accepted: 27 February 2014)

Abstract: Hafnium oxide thin films (HOTFs) were successfully deposited onto amorphous glasses using chemical bath deposition, successive ionic layer absorption and reaction (SILAR), and sol–gel methods. The same reactive precursors were used for all of the methods, and all of the films were annealed at 300°C in an oven (ambient conditions). After this step, the optical and structural properties of the films produced by using the three different methods were compared. The structures of the films were analyzed by X-ray diffraction (XRD). The optical properties are investigated using the ultraviolet-visible (UV–VIS) spectroscopic technique. The film thickness was measured via atomic force microscopy (AFM) in the tapping mode. The surface properties and elemental ratios of the films were investigated and measured by scanning electron microscopy and energy-dispersive X-ray spectroscopy (EDX). The lowest transmittance and the highest reflectance values were observed for the films produced using the SILAR method. In addition, the most intense characteristic XRD peak was observed in the diffraction pattern of the film produced using the SILAR method, and the greatest thickness and average grain size were calculated for the film produced using the SILAR method. The films produced using SILAR method contained fewer cracks than those produced using the other methods. In conclusion, the SILAR method was observed to be the best method for the production of HOTFs.

Keywords: hafnium oxide; thin films; optical properties; structural properties; chemical deposition; absorption; sol–gel process

1. Introduction

Researchers are currently interested in hafnium oxide because of its electrical properties. The main reason for replacing silicon dioxide in metal oxide transistors with hafnium oxide is that the latter has a high dielectric constant [1–2]. Moreover, with its monoclinic structure, hafnium oxide exhibits a high optic gap width of approximately 5.5 to 6 eV. Because of these features, hafnium oxide stands out as a material that is well suited for use in optoelectronic devices [3–5]. Martinez *et al.* [6] have noted that, although the literature contains few studies related to the optical properties of hafnium oxide thin films (HOTFs), HfO_2 may have interesting optical applications. Because of its large band gap and high refractive index, HfO_2 has been used as optical coatings for astronomical charge coupled devices (CCDs) and as anti-reflective multilayer coatings for night-vision devices and infrared (IR) optical devices. The optical properties of hafnium oxide are useful because of its corresponding electrical properties [6].

Researchers have attempted to produce hafnium oxide using various methods such as atomic layer deposition [7], sol–gel process [8], metal–organic chemical vapor deposition [9], magnetic sputtering [10], and spin coating [11], and they continue to develop new methods of producing it. The main problem lies in the necessity of using several devices required for the application of most of these methods. The most economical methods for producing thin films are those in which production occurs as a result of a chemical reaction in an aqueous solution. Chemical bath deposition (CBD), successive ionic layer absorption and reaction (SILAR), and sol–gel process are the most commonly used methods; all of these methods are cheap and easily applicable techniques. The only requirement for using these methods is the knowledge of chemistry of the process. Because the preparation of metal oxides at low temperature in aqueous reactions is difficult, these methods are not well suited for the preparation

Corresponding author: İ.A. Kariper E-mail: akariper@gmail.com

of metal oxide thin films. Thus, researchers have attempted to solve this problem by annealing sulfur or organic composites of metals adhered to the surface in gel form.

In this study, we discussed the best method for the production of HOTFs, which is significant in the world of materials, using simple and economical production methods—specifically, the CBD, SILAR, and sol–gel process. We researched which method is more useful than the others for researchers.

2. Experimental

2.1. Materials

The stock solutions were prepared using highly pure compounds (99.9%, E. Merck, Darmstadt, Sigma-Aldrich). All laboratory glassware and substrates were cleaned by soaking in diluted nitric acid and rinsing with alcohol and deionized water.

2.2. Preparation of HOTFs

CBD: 0.01 mol, 0.030 L of $HfCl_4$ (0.01 mol of $HfCl_4$ dissolved in 0.030 L of water) was mixed with 0.02 mol, 0.030 L of thioacetamide in a beaker. Amorphous glass substrates, which had been washed with detergent and rinsed with distilled water, were dipped into the beaker. 10 mL of KOH solution (pH 12) was added to this chemical bath. The bath was placed in an oven and maintained at 70°C for 1 h. The substrates were washed with distilled water after being removed from the beaker and were subsequently annealed for 3 h at 300°C.

SILAR: 0.01 mol, 0.030 L of $HfCl_4$ (0.01 mol of $HfCl_4$ dissolved in 0.030 L of water) was placed in a beaker, and 0.030 L, 0.02 mol of sodium sulfide solution was prepared in another beaker. Amorphous glass substrates, which had been washed with detergent and rinsed with distilled water, were first dipped into the $HfCl_4$ solution and then into the sodium sulfide solution. This dipping application was performed eight times. The substrates were washed with distilled water after being removed from the beaker and were subsequently annealed for 3 h at 300°C.

Sol–gel: 0.01 mol, 0.010 L of $HfCl_4$ (0.01 mol of $HfCl_4$ dissolved in 0.010 L of water) was mixed with 0.030 L of concentrated glycerin in a beaker. Amorphous glass substrates, which had been washed with detergent and rinsed with distilled water, were dipped into the beaker eight times. They were subsequently washed with distilled water after being removed from the beaker and were annealed at 300°C for 3 h.

2.3. Characterization techniques

The crystalline structure of HfO_2 was confirmed by X-ray diffraction (XRD) on a diffractometer equipped with a Cu $K_{\alpha 1}$ radiation source (Rikagu RadB, λ = 0.15406 nm); the samples were scanned over the range $10° \leq 2\theta \leq 90°$ at a speed of $3°{\cdot}min^{-1}$ and with a step size of 0.02°. The surface properties of the films were investigated using an EVO40-LEO computer-controlled digital scanning electron microscope (SEM). Energy-dispersive X-ray spectroscopy (EDX) chemical analysis was performed with an EDX spectrometer attached to the SEM. Optical measurements were performed on a Hach Lange 5000 spectrophotometer at room temperature by placing an uncoated identical commercial glass substrate in the reference beam. The optical spectra of thin films were recorded in wavelength at a range of 300–1100 nm. Film thicknesses were measured over a 10 μm × 10 μm area in the tapping mode and were determined with a Veeco Multi-Mode atomic force microscope equipped with a NanoScope 3D controller.

3. Results and discussion

Chemical reactions that occurred during the bath deposition are summarized below.

CBD:

$$Hf^{4+} + 4H_2O + 4CH_3CSNH_2 \rightarrow HfS_4 + 4CH_3CONH_2 + 8H^+ + 4e^- \quad (1)$$

$$HfS_4 + 5O_2 \xrightarrow{300°C} HfO_2 + 4SO_2 \quad (2)$$

SILAR:

$$Hf^{4+} + 4S^{2-} \rightarrow HfS_4 + 4e^- \quad (3)$$

$$HfS_4 + 5O_2 \xrightarrow{300°C} HfO_2 + 4SO_2 \quad (4)$$

Sol–gel process:

$$Hf^{4+} + 4e^- + C_3H_8O_3 \rightarrow Hf\{C_3H_8O_3\}_{(sol-gel)} \quad (5)$$

$$Hf\{C_3H_8O_3\}_{sol-gel} + 9/2O_2 \xrightarrow{300°C} HfO_2 + 3CO_2 + 4H_2O \quad (6)$$

Eqs. (1) and (2) show the formation of HfO_2 via the CBD method, Eqs. (3) and (4) show the formation of HfO_2 via the SILAR method, and Eqs. (5) and (6) show the formation of HfO_2 via the sol–gel method.

Fig. 1 displays the XRD patterns of various HOTFs produced via the CBD, SILAR, and sol–gel methods. A comparison of some peaks in these XRD patterns with ASTM values is presented in Table 1. Data presented here are raw data; no cleaning or smoothing was performed so that researchers can choose the best method among them. In the case of the film prepared via the sol–gel method, the observed structure was almost amorphous; however, the most

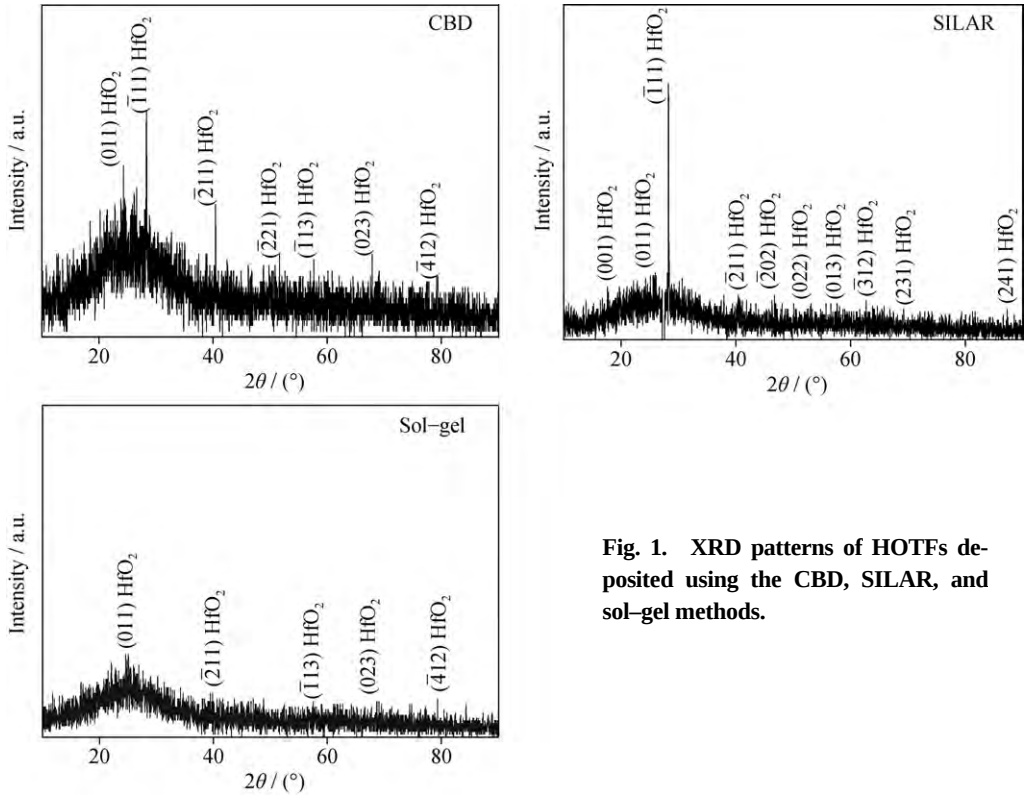

Fig. 1. XRD patterns of HOTFs deposited using the CBD, SILAR, and sol–gel methods.

Table 1. XRD data of ASTM values for various films

Chemical bath deposition				
ASTM data file	ASTM value / (°)	Observed value / (°)	Miller index	Structure
78-500	24.189	24.232	HfO_2 (011)	Monoclinic
78-500	28.347	28.341	HfO_2 ($\bar{1}$11)	Monoclinic
34-104	40.185	40.425	HfO_2 ($\bar{2}$11)	Monoclinic
78-500	51.535	51.633	HfO_2 ($\bar{2}$21)	Monoclinic
34-107	57.535	57.735	HfO_2 ($\bar{1}$13)	Monoclinic
34-107	66.318	67.825	HfO_2 (023)	Monoclinic
34-107	79.188	79.153	HfO_2 ($\bar{4}$12)	Monoclinic
SILAR				
ASTM data file	ASTM value / (°)	Observed Value/ (°)	Miller index	Structure
34-104	17.544	17.632	HfO_2 (001)	Monoclinic
78-500	24.189	24.232	HfO_2 (011)	Monoclinic
78-500	28.347	28.260	HfO_2 ($\bar{1}$11)	Monoclinic
34-104	40.185	40.305	HfO_2 ($\bar{2}$11)	Monoclinic
34-104	45.783	46.768	HfO_2 ($\bar{2}$02)	Monoclinic
34-104	50.436	50.137	HfO_2 (022)	Monoclinic
34-104	57.535	57.614	HfO_2 (013)	Monoclinic
34-104	62.350	62.720	HfO_2 (312)	Monoclinic
34-104	69.367	69.183	HfO_2 (231)	Monoclinic
34-104	87.534	87.370	HfO_2 (241)	Monoclinic
Sol–gel process				
ASTM data file	ASTM value/ (°)	Observed value/ (°)	Miller index	Structure
78-500	24.189	24.611	HfO_2 (011)	Monoclinic
34-104	40.185	40.047	HfO_2 ($\bar{2}$11)	Monoclinic
34-107	57.535	57.614	HfO_2 ($\bar{1}$13)	Monoclinic
34-107	66.318	67.688	HfO_2 (023)	Monoclinic
34-107	79.188	79.394	HfO_2 ($\bar{4}$12)	Monoclinic

intense peak was observed in the pattern of the film prepared via the SILAR method. Thus, the SILAR method and the prepared bath can be used as a specific methodology for the preparation of HOTFs. The peaks of XRD patterns show the formation of a phase, which is hafnium oxide, with a monoclinic structure [12]. The XRD results were consistent with standard ASTM values.

The grain size (D), which is a structural parameter, was determined for all of the films based on their XRD patterns; the results are presented in Fig. 2. The film thickness, as measured by atomic force microscopy (AFM), is also presented in Fig. 2. The grain size of the thin films was calculated from the XRD patterns using the Scherrer formula:

$$D = \frac{0.9\lambda}{B\cos\theta} \tag{7}$$

where D is the grain size, λ is the X-ray wavelength, β is the angular line width at half-maximum intensity (in radians), and θ is the Bragg angle. The grain size of the films was calculated by using the FWHM of the $(\bar{1}11)$ peak in the case of the film prepared via the SILAR method, the $(\bar{1}11)$ peak for the film prepared via the CBD method, and the (011) peak in the case of the film prepared via the sol–gel method, and was obtained through Scherrer's method, which takes the highest-intensity peaks of the XRD patterns.

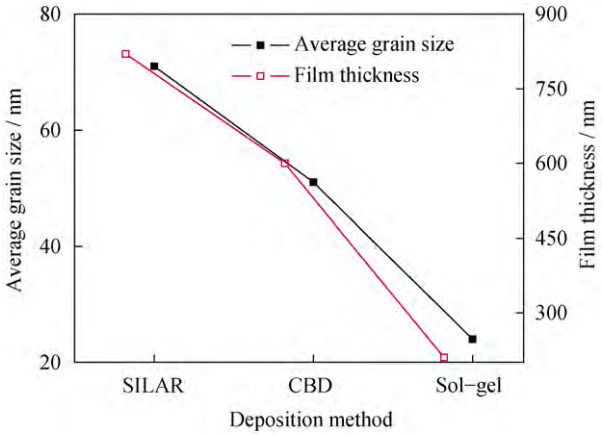

Fig. 2. Average grain size and film thickness of HOTFs deposited using the CBD, SILAR, and sol–gel methods.

The HOTF with the largest average grain size was obtained via the SILAR method. The average grain sizes of the thin films were 71, 51, and 24 nm for the films prepared via the SILAR, CBD, and sol–gel methods, respectively. It is understood that small grain size was prepared via the sol–gel method, which has low intensity of its XRD peaks. As the average grain size decreases, the grains stock up more tightly, this causes a decrease in the volumes of the spaces between grains. Thus, the deposition of a film with a smaller grain size leads to a more orderly structure. This effect can also be observed in the XRD patterns of the films. Therefore, the peaks that we observed in the XRD pattern of the film prepared via the SILAR method have higher intensities than other methods. The film thicknesses of the films were 820, 600, and 210 nm for the films prepared using the SILAR, CBD, and sol–gel methods, respectively. The thicknesses of the films are consistent with their average grain sizes [13]. Of course, the film thickness and the average grain size depend on the deposition time, the deposition temperature, and the nature of the precursor, even though the concentrations of the precursors were similar in our experiments.

The transmittance (T) of the HOTFs was calculated on the basis of the reflectivity (R) and absorbency (A) using the following expression:

$$T = (1-R)^2 e^{-A} \tag{8}$$

Figs. 3 and 4 show the transmittance and reflectance of HOTFs obtained using the SILAR, CBD, and sol–gel methods. The lowest transmittance and the highest reflectivity

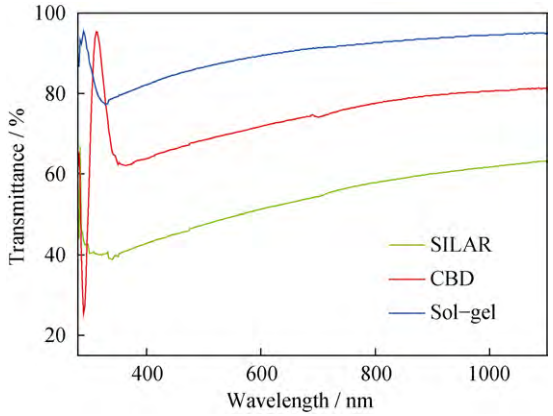

Fig. 3. Transmittance of HOTFs deposited using the SILAR, CBD, and sol–gel methods.

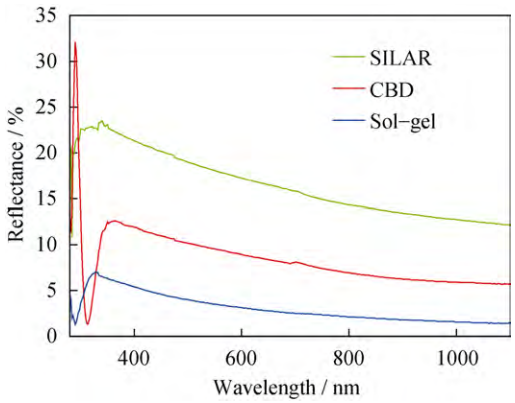

Fig. 4. Reflectance of HOTFs deposited using the SILAR, CBD, and sol–gel methods.

values were observed for the films prepared using the SILAR method [6] because the absorption of light by its crystal structure was the greatest among the prepared films. The transmittance decreases as the absorption increases, and film thickness affects the transmittance and reflectance curves.

The refraction indexes (n) and extinction coefficients (k) of the films were calculated using the following formula:

$$n = \frac{1+R}{1-R} + \sqrt{\frac{4R}{(1-R)^2} - k^2} \tag{9}$$

The refraction indexes are presented in Fig. 5. The refraction indexes of HOTFs paralleled the average grain size and thickness of the films. The refraction indexes of HOTFs deposited using the SILAR, CBD and sol–gel methods were calculated to be 2.47, 1.89, and 1.46, respectively, at a wavelength of 550 nm. In addition, the average grain sizes of HOTFs deposited using the SILAR, CBD and sol–gel methods were calculated to be 71, 51, and 24 nm, respectively. The values of refraction indexes and extinction coefficients exhibited natural behavior. Because the refraction of light is greater in a scattered structure, the refraction index is higher for large grains. The refractive indexes are consistent with values reported in Refs. [14–15].

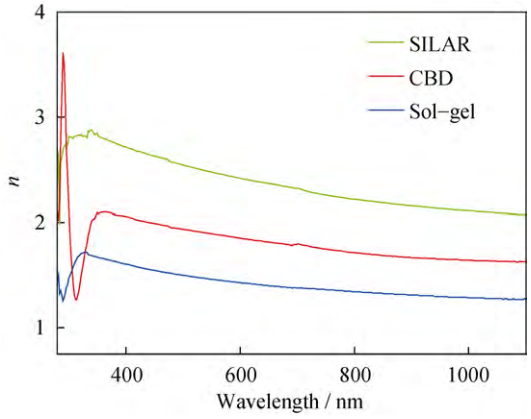

Fig. 5. Refraction index of HOTFs deposited using the CBD, SILAR, and sol–gel methods.

As expected, the EDX and SEM analyses indicate that HOTFs produced using the SILAR method are with a higher quality than those produced using the other two methods. This result is based on hafnium content in the structures of the films.

Fig. 6 presents the EDX spectra for the prepared films. The reason that the films prepared using the SILAR method exhibit the highest hafnium ratio is that thioacetamide was detached from the structure of the SILAR films at approximately 300°C, because of removal of organic contaminations as evident in the analysis results. In the case of the films prepared using the sol–gel method, glycerin was not detached from the structure at the annealing temperature and resulted in impurities, as indicated by low hafnium ratio in the EDX analysis of these films. Thus, the oxidation of hafnium sulfide in the films produced using the SILAR method, even at low annealing temperature, makes this method advantageous compared to the other methods. We determined that the level of contamination by organic compounds is quite high in the films prepared using the CBD and sol–gel methods. The hafnium ratios of the films prepared using the SILAR, CBD, and sol–gel methods, as determined by EDX analysis, were 82.73wt%, 63.44wt%, and 34.76wt%, respectively. In theory, this ratio should be 84.76wt% hafnium and 15.24wt% oxygen. The result closest to the theoretical value was observed for the films produced using SILAR method.

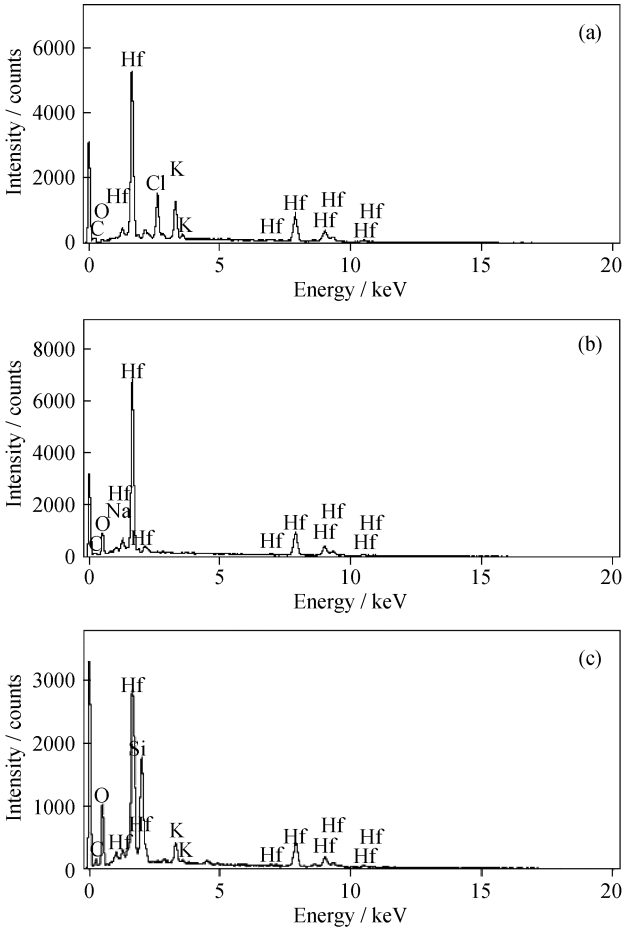

Fig. 6. EDX spectra of HOTFs prepared using the CBD (a), SILAR (b), and sol–gel (c) methods.

The SEM images are presented in Fig. 7. In general, cracks were observed in the films. These cracks cause an increase in the gaps between particles, which allows us to observe, via XRD analysis, the amorphous structure of the glass that was used as the substrate. The increase in these

cracks may cause a deformation in the structure and an increase in the electrical resistance of the material. Of course, these films are quite adequate as porous materials. The largest cracks were observed in the films produced using the sol–gel method, whereas a denser structure was observed in the film produced by using the SILAR method. The transmittance increases with increasing structure density, and denser structures absorb more light than cracked or porous structures. Therefore, we observed low transmittance in the film prepared using the SILAR method. Similarly, we observed high reflectance in the films prepared using the SILAR method. As noted in Refs. [16–17], the chemical method is very advantageous in terms of cost. The films could be washed with organic solvents to remove organic contaminations, but this approach would result in solvent contamination.

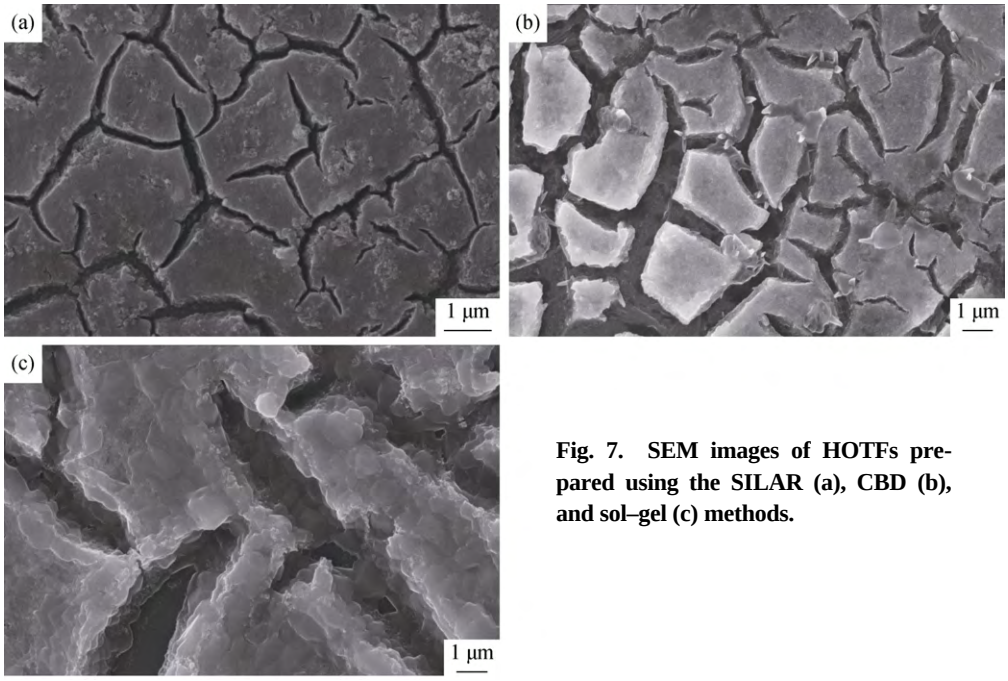

Fig. 7. SEM images of HOTFs prepared using the SILAR (a), CBD (b), and sol–gel (c) methods.

4. Conclusions

In this study, we produced HOTFs using three different methods to identify a method for producing good-quality HOTFs. The SILAR, CBD, and sol–gel methods, which are economical, simple, and do not require additional devices, were selected for this purpose. The knowledge of chemistry of the processes was sufficient for the application of these methods. With respect to the XRD analysis results, we observed the sharpest peaks in the patterns of the films prepared using the SILAR method. The average grain sizes of the thin films were 71, 51, and 24 nm for the films prepared using the SILAR, CBD, and sol–gel methods, respectively, and their respective film thicknesses were 820, 600, and 210 nm. The results of EDX and SEM analyses revealed that the highest-quality films were produced via the SILAR method. The films produced using the SILAR method contained fewer cracks; EDX analysis further revealed that the films produced by using the SILAR method contained fewer impurities and exhibited the highest hafnium ratio among the investigated films. The hafnium ratios of the films determined by EDX analysis were 82.73wt%, 63.44wt%, and 34.76wt% for those produced using the SILAR, CBD, and sol–gel methods, respectively. Furthermore, the highest values of the reflection curve and refractive index were calculated for the film produced using the SILAR method. During the preparation of films by the other methods, the selected reagents were not volatilized at an annealing temperature of 300°C, which was the main disadvantage of these methods. The use of higher annealing temperatures and longer annealing times increased the quality of HOTFs produced with these methods; however, increasing the annealing temperature and extending the annealing time will also increase the production costs. Of course, all of the reagents and starting materials should be similar to allow a perfect comparison, but similar reagents and starting materials cannot be used in all methods. Thus, for each method, reagents used in previous processes reported in the literature or previously reported processes were used. From this viewpoint, the SILAR method appears to be the best method for the preparation of HOTFs.

References

[1] G.D. Wilk, R.M. Wallace, and J.M. Anthony, High-κ gate dielectrics: Current status and materials properties considerations, *J. Appl. Phys.*, 89(2001), No. 10, p. 5243.

[2] A.I. Kingdom, J.P. Maria, and S.K. Streiffer, Alternative dielectrics to silicon dioxide for memory and logic devices, *Nature*, 406(2000), p. 1032.

[3] P.E. Batson, Conduction bandstructure in strained silicon by spatially resolved electron energy loss spectroscopy, *Ultramicroscopy*, 59(1995), No. 1-4, p. 63.

[4] M.P. Agustin, G. Bersuker, B. Foran, L.A. Boatner, and S. Stemmer, Scanning transmission electron microscopy investigations of interfacial layers in HfO_2 gate stacks, *J. Appl. Phys*., 100(2006), art. No. 024103.

[5] D.A. Muller, T. Sorsch, S. Moccio, F.H. Baumann, K. Evans-Lutterodt, and G. Timp, The electronic structure at the atomic scale of ultrathin gate oxides, *Nature*, 399(1999), p. 758.

[6] F.L. Martinez, M. Toledano-Luque, J.J. Gandia, J. Cárabe, W. Bohne, J. Röhrich, E. Strub, and I. Mártil, Optical properties and structure of HfO_2 thin films grown by high pressure reactive sputtering, *J. Phys. D*, 40(2007), p. 5256.

[7] M.C. Cheynet, S. Pokrant, F.D. Tichelaar, and J.L. Rouvière, Crystal structure and band gap determination of HfO_2 thin films, *J. Appl. Phys*., 101(2007), art. No. 054101.

[8] H. Kozuka, *Handbook of Sol–Gel Science and Technology Processing, Characterization and Applications*, Kluwer Academic Publishers, New York, 2005, p. 247.

[9] N.V. Nguyen, A.V. Davydov, and D. Chandler-Horowitz, Sub-bandgap defect states in polycrystalline hafnium oxide and their suppression by admixture of silicon, *Appl. Phys. Lett.*, 87(2005), art. No. 192903.

[10] G. He, L.Q. Zhu, M. Liu, Q. Fang, and L.D. Zhang, Optical and electrical properties of plasma-oxidation derived HfO_2 gate dielectric films, *Appl. Surf. Sci*., 253(2007), No. 7, p. 3413.

[11] K. Jiang, J.T. Anderson, K. Hoshino, D. Li, J.F. Wager, and D.A. Keszler, Low-energy path to dense HfO_2 thin films with aqueous precursor, *Chem. Mater*., 23(2011), No. 4, p. 945.

[12] A.R. Teren, R. Thomas, J.Q. He, and P. Ehrhart, Comparison of precursors for pulsed metal–organic chemical vapor deposition of HfO_2 high-K dielectric thin films, *Thin Solid Films*, 478(2005), No. 1-2, p. 206.

[13] X. Zhang, X.H. Song, and D.L. Zhang, Thickness dependence of grain size and surface roughness for dc magnetron sputtered Au films, *Chin. Phys. B*, 19(2010), No. 8, art. No. 086802.

[14] H. Shimizu, D. Nemoto, M. Ikeda, and T. Nishide, Characteristics of sol–gel-derived and crystallized HfO_2 thin films dependent on sol solution, *Jpn. J. Appl. Phys.*, 49(2010), art. No. 121502.

[15] H. Hu, C.X. Zhu, Y.F. Lu, Y.H. Wu, T. Liew, M.F. Li, B.J. Cho, W.K. Choi, and N. Yakolev, Physical and electrical characterization of HfO_2 metal–insulator–metal capacitors for Si analog circuit applications, *J. Appl. Phys.*, 94(2003), No. 1, p. 551.

[16] İ.A. Kariper and T. Özpozan, Cobalt xanthate thin film with chemical bath deposition, *J. Nanomater.*, 2013(2013), art. No. 139864.

[17] H.M. Pathan and C.D. Lokhande, Deposition of metal chalcogenide thin films by successive ionic layer adsorption and reaction (SILAR) method, *Bull. Mater. Sci.*, 27(2004) No. 2, p. 85.